

ORIGINAL ARTICLE

Meloxicam synergistically enhances the *in vitro* effects of sunitinib malate on bladder-cancer cells

Regina Arantes-Rodrigues¹, Rosário Pinto-Leite², Lio Fidalgo-Gonçalves³, Isabel Gaivão⁴, Aura Colaço¹, Paula Oliveira¹, Lúcio Santos⁵

¹Department of Veterinary Sciences, CECAV, University of Trás-os-Montes and Alto Douro, Vila Real, Portugal

²Genetic Service, Cytogenetic Laboratory, Hospital Center of Trás-os-Montes and Alto Douro, Vila Real, Portugal

³Department of Engineering, CMUTAD, University of Trás-os-Montes and Alto Douro, Vila Real, Portugal

⁴Department of Genetics and Biotechnology, CECAV, University of Trás-os-Montes and Alto Douro, Vila Real, Portugal

⁵Experimental Pathology and Therapeutics Group, Portuguese Institute of Oncology, Porto, Portugal

Received 31st December 2012.

Revised 2nd January 2013.

Published online 8th January 2013.

Summary

To evaluate the *in vitro* effects of sunitinib malate and meloxicam in isolation, and to analyse the ability of meloxicam to enhance the cytotoxicity of sunitinib malate in three human bladder-cancer cell lines. Cell lines were treated with sunitinib malate and meloxicam, either in isolation or combined. Leishman staining, MTT method, comet assay, MDC staining and M30 CytoDEATH antibody were performed. The Chou and Talalay method was applied. Sunitinib malate and meloxicam suppressed cell proliferation in bladder-cancer cells in isolation, in a concentration-dependent manner. Treatment of bladder-cancer cells with a combination of sunitinib malate and meloxicam showed a synergistic effect. When exploring the mechanism of this combination by means of comet assay, there is the suggestion that meloxicam increases sunitinib malate cytotoxicity through DNA damage. Autophagic and apoptotic studies show a greater incidence of autophagic vacuoles and early apoptotic cells when the combined treatment was put into use. In isolation, sunitinib malate and meloxicam demonstrated anti-tumour effects in our study. Furthermore, simultaneous exposure of cells to sunitinib malate and meloxicam provided a combinatorial beneficial effect. This hints at the possibility of a new combined therapeutic regimen, which could lead to improvements in the treatment of patients with bladder cancer.

Key words: bladder cancer; bladder-cancer cell lines; sunitinib malate; meloxicam; synergistic

INTRODUCTION

Currently accepted for use in the treatment of advanced renal cancer, sunitinib malate is an oral, multi-targeted receptor tyrosine kinase inhibitor of

the vascular endothelial growth factor receptor 1-3, platelet-derived growth factor receptor, stem cell receptor, and FMS-like tyrosine kinase-3 receptor (Wiedenmann et al. 2011). Sunitinib malate has the ability to both regulate tumour growth and to block angiogenesis (Ping et al. 2012). The therapeutic effects of sunitinib malate on bladder cancer have already been assessed in two clinical studies of phase II cancers and shown clinical benefits (Gallagher et al. 2010, Bellmunt et al. 2011). Chronic inflammation precedes most cancers and is considered a “hallmark” of the neoplastic process, including in cases of bladder cancer (Michaud 2007). An intrinsic pathway of this inflammation is driven

✉ Paula Oliveira, Department of Veterinary Sciences, CECAV, University of Trás-os-Montes and Alto Douro, Vila Real 5001-801, Portugal

✉ pamo@utad.pt

☎ 351 966473062

☎ 351 259350480

by cells transformed by several genetic events: the tumour-initiating cells. A second pathway, which includes external inflammatory conditions, further increases the risk of developing cancer. These two pathways activate transcription factors that lead to the overexpression, elevated secretion or abnormal activation of pro-inflammatory mediators such as cytokines, chemokines, cyclooxygenase-2 (COX-2), prostaglandins, inducible nitric oxide synthase (iNOS) and nitric oxide (Karin 2006). For this reason, anti-inflammatory drugs may have a role to play in bladder-cancer therapies.

Non-steroidal anti-inflammatory drugs (NSAIDs) are commonly prescribed to treat inflammatory conditions and pain (Scheiman and Hindley 2010). The cyclooxygenase (COX) pathway represents the specific target of NSAIDs. COX enzymes are responsible for catalyzing the conversion of arachidonic acid into prostaglandins, which are involved in a diverse range of physiological processes, notably inflammation. Currently, there are three known isoforms of cyclooxygenases (COX-1, COX-2 and COX-3). COX-1 represents the constitutive form, it is expressed in many tissues (kidneys, intestine, platelets and stomach) (Hamama et al. 2005) and is responsible for several physiological functions (gastric mucosa integrity, platelet function and maintaining normal renal functions) (Compare et al. 2010). COX-3 is described as a novel COX-1 variant, also denominated as COX-1b. However, the specific role of COX-3 in humans has not yet been fully described (Chandrasekharan et al. 2002). COX-2 is the only isoform that has been associated with carcinogenesis (Williams et al. 1999), given that it is expressed in several malignant tumours (Eberhart et al. 1994, Gupta et al. 2000, Hwang et al. 1998, Watkins et al. 1999) including in bladder-cancer cells (Dhawan et al. 2008). The therapeutic effects of selective COX-2 inhibitors have already been assessed in *in vivo* (human hepatocellular carcinoma implants in nude mice) and in *in vitro* (canine osteosarcoma cells) models with encouraging outcomes (Kern et al. 2004, Wolfesberger et al. 2006). Developed in 1977, meloxicam, a derivative of enolic acid, is a NSAID widely used with anti-inflammatory, antipyretic and analgesic properties. Meloxicam exerts its effects through the inhibition of the COX-2 enzyme (Furst 1997). Several reports suggest that meloxicam has anti-tumour properties in different cancer cell lines, such as prostate (Montejo et al. 2010), colorectal (Goldman et al. 1998) and non-small lung cancer cells (Tsubouchi et al. 2000), as well as, in animal models (Kern et al. 2004, Tsuchida et al. 2005). Nevertheless, the effect of meloxicam on *in vivo* and *in vitro* models of bladder cancer is still lacking.

Bladder cancer remains one of the most established diseases in the Western world (Jacobs et al. 2012). The number of treatment options has increased during recent years, but chemotherapy courses continue to produce unsatisfactory rates of recurrence and death.

In this study, we evaluate the *in vitro* effects of sunitinib malate and meloxicam in isolation, and the combined effects of using both drugs, on HCV29 human normal urothelial cells and on T24, 5637 and HT1376 human bladder-cancer cell lines.

MATERIALS AND METHODS

Drugs

Sunitinib malate was acquired from Sigma Aldrich (St. Louis, EUA). This was dissolved in distilled water to create a stock solution of 1 mM that was stored at -20°C . Meloxicam was obtained from Boehringer Ingelheim (Lisboa, Portugal) and it was prepared in culture medium.

Cell culture conditions

HCV29 human normal urothelial cells were kindly provided by Dr. Mónica Botelho of the Centre for Parasite Immunology and Biology (National Institute of Health, Porto, Portugal). Three human bladder-cancer cell lines were used for the experiments: T24 and HT1376 (two muscle-invasive cell lines) and 5637 (a non-muscle-invasive cell line). T24 cell line was provided by DSMZ, Düsseldorf, Germany. 5637 and HT1376 cell lines were provided by Dr. Paula Videira of the Universidade Nova de Lisboa. HCV29 cells were grown as monolayers in RPMI 1640 culture medium (PAA, Pasching, Austria) containing 10% fetal bovine serum (Biological Industries, Kibbutz Beit Haemek, Israel), 100 U/ml penicillin (Biological Industries), 100 $\mu\text{g}/\text{ml}$ streptomycin (Biological Industries) and 2 mM L-glutamine (Sigma Aldrich, St. Louis, MO). T24, 5637 and HT1376 cells were cultured at the same conditions but in culture medium containing 10% heat-inactivated fetal bovine serum. The cultures were maintained in a humidified 5% CO_2 incubator at 37°C .

Sunitinib malate and meloxicam exposure

HCV29 normal urothelial cells were exposed to several concentrations of sunitinib malate (1, 2, 4 and 6 μM) and meloxicam (50, 100, 200 and 400 μM). T24, 5637 and HT1376 bladder-cancer cells were exposed to sunitinib malate (1, 2, 4, 6 and 20 μM) and meloxicam (50, 100, 200, 400, 600 and 800 μM), over the course of 72 h to assess concentration-response profiles, in isolation or combined. For the combined

assays, the lowest concentration of sunitinib malate (1 μ M) was used simultaneously with 100 μ M of meloxicam. Cells growing in the complete medium alone were processed in the same way as the treated cells, in the case of all the methodologies, and cytotoxic effects were analyzed immediately after drug exposure was ceased. All the various dilutions of both drugs were freshly prepared in culture medium before each experiment.

Cell morphology

To analyze the presence of possible morphological alterations induced by sunitinib malate (1 μ M) and meloxicam (100 μ M), both in isolation and combined, a Leishman staining was performed after 72 h of drug incubation. Cells were seeded in glass coverslips (8 mm) and incubated overnight. At the end of treatment, cells were washed twice with phosphate-buffered saline (PBS) (pH 7.4, previously heated at 37 °C), fixed in methanol for 20 min at room temperature, washed once more with PBS and stained with Leishman dye for 30 min in the dark. After being washed with distilled water, cells were analysed with a light microscope (Leica DM750) (original magnification 1000X).

3-(4,5-dimethylthiazol-2-yl)-2,5-diphenyl tetrazolium bromide (MTT) assay

HVC29 normal urothelial cells and bladder-cancer cells resuspended in culture medium at a density of 2×10^4 cells/ml were seeded into each well of a 96-well flat-bottom microtiter (Sarstedt, Newton, NC) and allowed to adhere overnight. Cells were then exposed to sunitinib malate and meloxicam, in isolation and combined. At the end of the treatment, cell proliferation was assessed by using a system based MTT (Sigma Aldrich). Ten μ l of MTT dye-working solution (5 mg/ml) was added to each well for 4 h. The medium was removed and the formazan crystals generated were solubilized by adding 100 μ l/well of dimethylsulfoxide (Sigma Aldrich) for 5 min. Absorbance values at 492 nm were determined using an ELISA reader (Multiskan EX, Labsystems). The percentage of cell proliferation was calculated as: (absorbance of treated cells/absorbance of untreated cells) X 100.

Drug combination studies

For the study of synergism between sunitinib malate and meloxicam on cell growth inhibition of T24, 5637 and HT1376 cells, a combination index (CI) was performed using the data obtained from MTT assay. Drug combination studies were based on concentration-effect curves generated as a plot of the fraction of unaffected (proliferating) cells versus drug

concentration, in accordance to the Chou and Talalay (1984) method, using the CI equation: $CI = (D_1 / (Dx)_1) + (D_2 / (Dx)_2) / (D_1 / (Dx)_1 + D_2 / (Dx)_2)$, where $(D)_1$ and $(D)_2$ are the concentrations of sunitinib malate and meloxicam that exhibit a determined effect when applied simultaneously to the cells and $(Dx)_1$ and $(Dx)_2$ are the concentrations of the same drugs that exhibit the same determined effect when used in isolation. The CI values indicates a synergistic effect when <1 , an antagonistic effect when >1 and an additive effect when equal to 1.

Comet assay

DNA damage induced by use of sunitinib malate and meloxicam on normal urothelial cells and bladder-cancer cells was determined by comet assay. Untreated cells and cells exposed to sunitinib malate (1 μ M) and meloxicam (100 μ M), in isolation or combined, were trypsinized, washed in ice-cold PBS and centrifuged at 500 X g for 5 min. Cell suspensions were resuspended in 140 μ l of 1% low-melting point agarose (Invitrogen Life Technologies, UK) diluted in PBS and were then dispensed onto two pairs of 70 μ l gels on glass microscopic slides (previously precoated with 1% normal melting point agarose and dried), covered with an 18 \times 18 mm cover slip and kept for 5 min at 4 °C to solidify. Cover slips were removed and slides were immersed in freshly prepared ice-cold lysing buffer (2.5 M NaCl, 100 mM Na₂EDTA, 10 mM Tris, 1% (v/v) Triton X-100) and incubated at 4 °C for 1 h. Slides were placed in an electrophoresis chamber filled with freshly prepared cold alkaline electrophoresis buffer (1 mM EDTA, 0.3 N NaOH) and immersed for 40 min. Electrophoresis was performed for 20 min at 25 V and 300 mA. Neutralisation was accomplished by washing the slides three times with distilled water. Using a Nikon Eclipse E400 fluorescent microscope (Tokyo, Japan) (original magnification 200X), visual and computerized image analyses of DNA damage were performed in accordance with Collins et al. (2008). The DNA damage was quantified by means of the visual classification of nucleoids into five comet classes, according to tail intensity and length, from 0 (no tail) to 4 (almost all DNA in tail). The total score was expressed as arbitrary units (A.U.) on a scale of 0 to 400 per 100 scored nucleoids. A total of 50 comets on each gel were classified.

Monodansylcadaverine (MDC) staining

Autophagic vacuoles induced by sunitinib malate (1 μ M) and meloxicam (100 μ M) were evaluated using the auto-fluorescent substance MDC. Cells were seeded in a glass coverslip (8 mm), cultured for 24 h and treated with drugs, in isolation or combined,

for 72 h. The medium was removed and MDC (Sigma Aldrich) was added to the cells at 25 μM , at 37 $^{\circ}\text{C}$ and for 1 h. Subsequently, cells were washed three times with PBS and immediately analysed using a fluorescence microscope (Nikon Eclipse E400, Tokyo, Japan).

M30 CytoDEATH antibody assay

The M30 CytoDEATH antibody was applied to untreated and treated cells for the determination of early apoptotic events, by means of detecting the cytokeratin 18 that is present after cleavage by caspases. To do so, cells were seeded in a glass coverslip (8 mm) and incubated overnight. After this period, cells were treated with sunitinib malate (1 μM) and meloxicam (100 μM), in isolation or combined. After 72 h, cells were washed with PBS and fixed in methanol at -20°C for 30 min. After two washes with 0.1% Tween-20 in PBS, cells were incubated with M30 CytoDEATH antibody working solution (1:100) (Roche Diagnostics, Indianapolis, USA) for 30 min, at room temperature and in the dark. Following two

washing procedures with washing buffer, secondary Anti-Mouse-IgG-Fluorescein (10 $\mu\text{g}/\text{ml}$) antibody, diluted at 1:100 in incubation buffer, was added for 30 min. The last wash was performed with PBS. Glass coverslips were mounted in a slide with 4,6-diamidino-2-phenylindole (DAPI) (Vysis, Izasa) for visualization of cell nuclei. For the qualitative detection, fluorescence microscopy (Nikon Eclipse E400, Tokyo, Japan) analysis was used.

Statistical analysis

Statistical significance was determined using SPSS 17.0 statistical software (SPSS Inc. USA). An equality of variances was determined by using the Levene F test, and the difference between treatments and the control group was compared by Dunnett's Multiple Comparison post-hoc test. Data are expressed as mean \pm SD (SD = standard deviation). Test were calculated at the significance level $2\alpha=0.05$. Matlab software (version 7.9, R2009b) was used to determine the interaction between sunitinib malate and meloxicam.

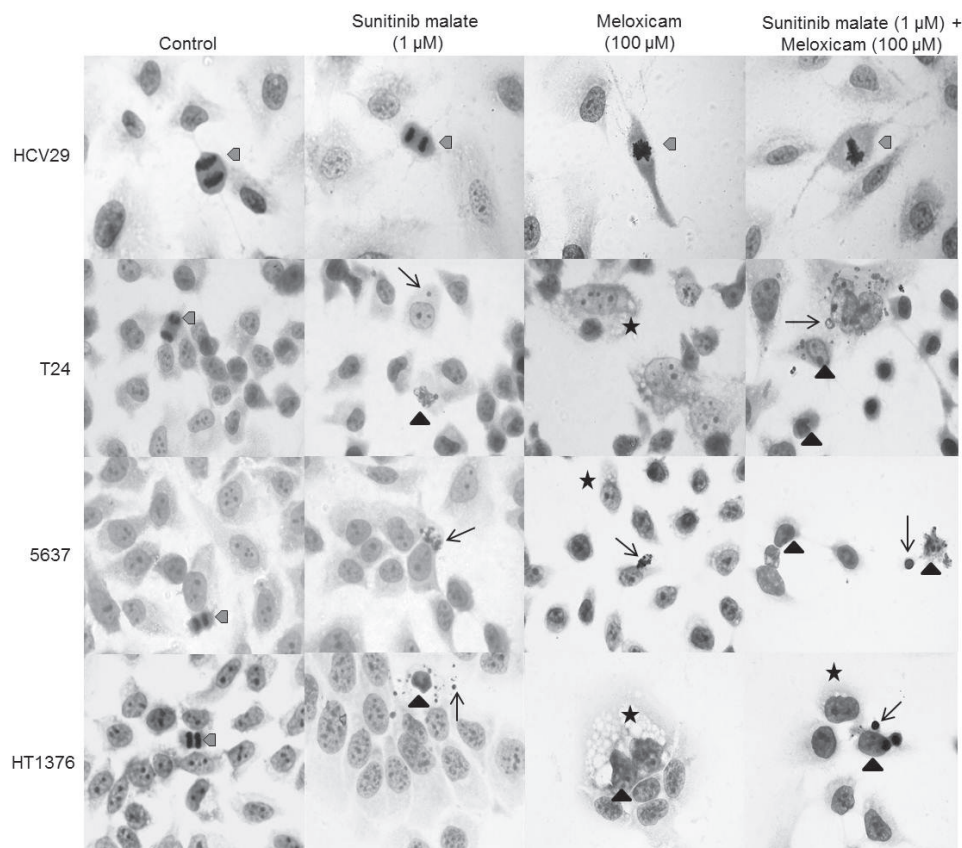


Fig. 1. Representative photomicrograph showing cultured HCV29, T24, 5637 and HT1376 bladder cell morphology. Apoptotic bodies (black arrow), cytoplasm vacuolization (asterisk) and apoptotic cells (triangle) were observed. Untreated cells show morphological characteristics of cells undergoing division (grey arrowhead). Original magnification 1000 \times .

RESULTS

Morphological studies

The morphological alterations observed on normal urothelial cells and bladder-cancer cells, after 72 h of culture in a mixture of sunitinib malate (1 μ M) and meloxicam (100 μ M), are schematically represented on Fig. 1. HCV29 untreated and treated cells did not present morphological alterations, with cells undergoing division in all the treatments. T24, 5637 and HT1376 untreated cells did not present any morphological changes, as it is possible to observe the intact nuclei and cells undergoing division in the three cell lines. Treatment of cells with sunitinib malate and meloxicam, in isolation, exhibited morphological features typical of apoptotic cells: shrinkage in cell size (accompanied by condensed chromatin), vacuolization of the cytoplasm and evidence of fragmentation of the nucleus into pieces of different sizes. In simultaneous exposure to both drugs, these characteristics were observed more frequently.

Isolated effects of sunitinib malate and meloxicam on cell proliferation

In order to be able to evaluate the effects of sunitinib malate and meloxicam in normal urothelial cells, the growth of HCV29 cell line was evaluated after exposure for 72 h to a wide range of concentrations of both drugs. From the results obtained we have found no evidence of inhibition cell proliferation after treatment with sunitinib malate (Fig. 2A) and meloxicam (Fig. 2B).

A panel of three bladder-cancer cell lines (T24, 5637 and HT1376) in the exponential growth phases were exposed to different concentrations of sunitinib malate (1, 2, 4, 6 and 20 μ M) and meloxicam (50, 100, 200, 400, 600 and 800 μ M), in isolation or combined, and the effect on cell proliferation was examined after 72 h of culture. Analysis of cell proliferation by using MTT assay reveals that sunitinib malate, in isolation, induced a concentration-dependent inhibitory effect on cell proliferation, with a very similar pattern response between the three cell lines (Fig. 2C). In the

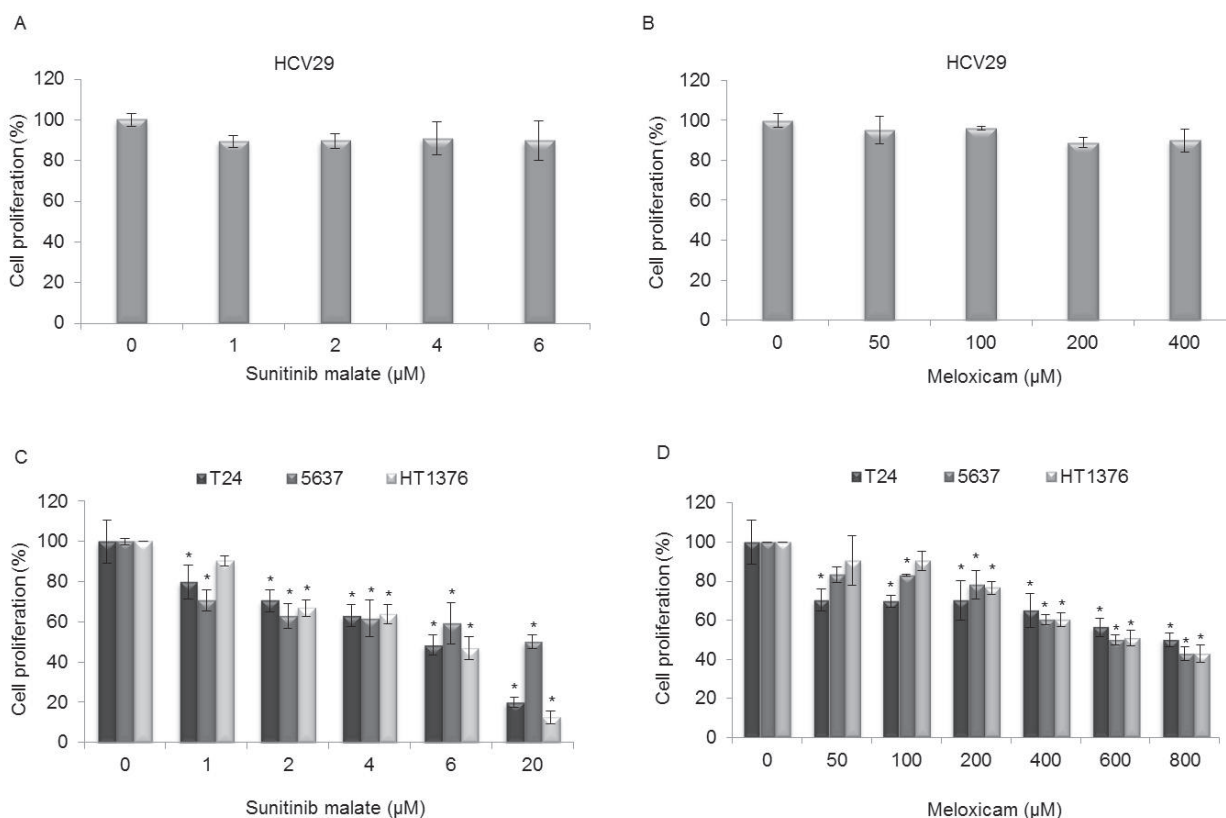


Fig. 2. MTT assay was performed to evaluate the differential sensitivity of HCV29 (A and B), T24, 5637 and HT1376 bladder-cancer cells to sunitinib malate (C) and meloxicam (D) in isolation, after 72 h of treatment. The data shown and the bars represent the mean values \pm SD. * Statistical significant compared with untreated cells.

presence of 1, 2, 4, 6 and 20 μM sunitinib malate, a cell proliferation-rate of 79.8, 70.4, 63, 48.5 and 20% for T24, 70.7, 62.9, 61.7, 59.2 and 51 for 5637 and 88.7, 63.8, 67, 50.9 and 12.5% for HT1376 cell line was obtained, respectively. The activity of sunitinib malate was statistical significant as compared with the control group (cells not treated), in the three cell lines, at all concentrations, with the exception of the HT1376 cell line at the lowest concentration tested (1 μM).

Fig. 2D shows the effects of meloxicam treatment obtained after bladder-cancer cell lines being exposed to increasing concentrations of the drug. A decrease in cell proliferation was obtained in the three cell lines used. A cell proliferation-rate of 70.2, 69.8, 70.1, 64.9, 56.4 and 50% on T24, 83.4, 82.9, 77.9, 60.4, 49.3 and 42.8% on 5637 and 90.5, 90.3, 76.6, 60.4, 51 and 43% on HT1376 cell line, was obtained in the presence of 50, 100, 200, 400, 600 and 800 μM meloxicam. Concerning the T24 cell line, a statistically significant reduction of cell proliferation was observed at all concentrations applied, compared with untreated cells. On the 5637 cell line at 50 μM , the cell-proliferation rate was not significant, as well as on the HT1376 cell line, at 50 and 100 μM . In the remaining concentrations, statistical significances were found when compared with untreated cells.

Combined effects of sunitinib malate and meloxicam on cell proliferation – combination index

The interactive effects between combinations of varying concentrations of sunitinib malate (1 μM to 6 μM) and meloxicam (50 μM to 400 μM) were evaluated by MTT assay. The simultaneous

treatment of sunitinib malate and meloxicam did not reduce HCV29 cell proliferation (Fig. 3A). The concomitant exposure of both drugs, over a wide range of concentrations and over three consequent days, decreased the cell-proliferation rate in the three bladder-cancer cell lines when compared with sunitinib malate cytotoxicity in isolation (Figs 3B, 3C and 3D). With the exception of 1 μM sunitinib malate plus 50 μM meloxicam on the 5637 cell line, all the remaining combinations are statistically significant compared with untreated cells.

In order to analyse the type of interaction (synergic, additive or antagonistic) between the several concentrations of sunitinib malate and meloxicam in combination at 72 h on T24, 5637 and HT1376 cell lines, we implemented on Matlab the method developed by Chou and Talalay (1984). Synergistic interactions occur when the combination index (CI) is below 1. The CI₅₀ values computed for T24, 5637 and HT1376 cell lines were 0.73, 0.75 and 0.94, respectively (Table 1). Therefore, the combined use of sunitinib malate and meloxicam was synergistic on the growth inhibition of the three cell lines (Fig. 4). Dose reduction index₅₀ (DRI₅₀) represents the magnitude of dose reduction obtained for the 50% growth inhibitory effect in combination setting as compared to each drug alone. In our experiments, the DRI₅₀ of sunitinib malate and meloxicam were equal to 5.69 and 2 in T24, 20 and 1.5 in 5637 and 6 and 1.5 in HT1376 cells, respectively, when the two drugs were used in combination (Table 1).

These results demonstrate that a synergistic interaction can be verified on cell proliferation when the two drugs are used in a simultaneous schedule.

Table 1. Combination index^a (CI) and dose reduction index^b (DRI) values for sunitinib malate and meloxicam combination. The analysis was performed using the method developed by Chou and Talalay (1984). The implementation was carried out on Matlab software.

Cell lines	Sunitinib malate (IC ₅₀ μM)	Meloxicam (IC ₅₀ μM)	CI ₅₀	DRI ₅₀	Interpretation
T24	5.69	800	0.73	Sunitinib malate: 5.69 Meloxicam: 2	Synergism
5637	20	600	0.75	Sunitinib malate: 20 Meloxicam: 1.5	Synergism
HT1376	6	600	0.94	Sunitinib malate: 6 Meloxicam: 1.5	Synergism

^a CI₅₀ is a “combination index” for 50% effect, used for quantifying synergism, additivity and antagonism; ^b DRI represents the order of magnitude (fold) of dose reduction obtained for IC₅₀ effect in combination setting as compared to each drug alone.

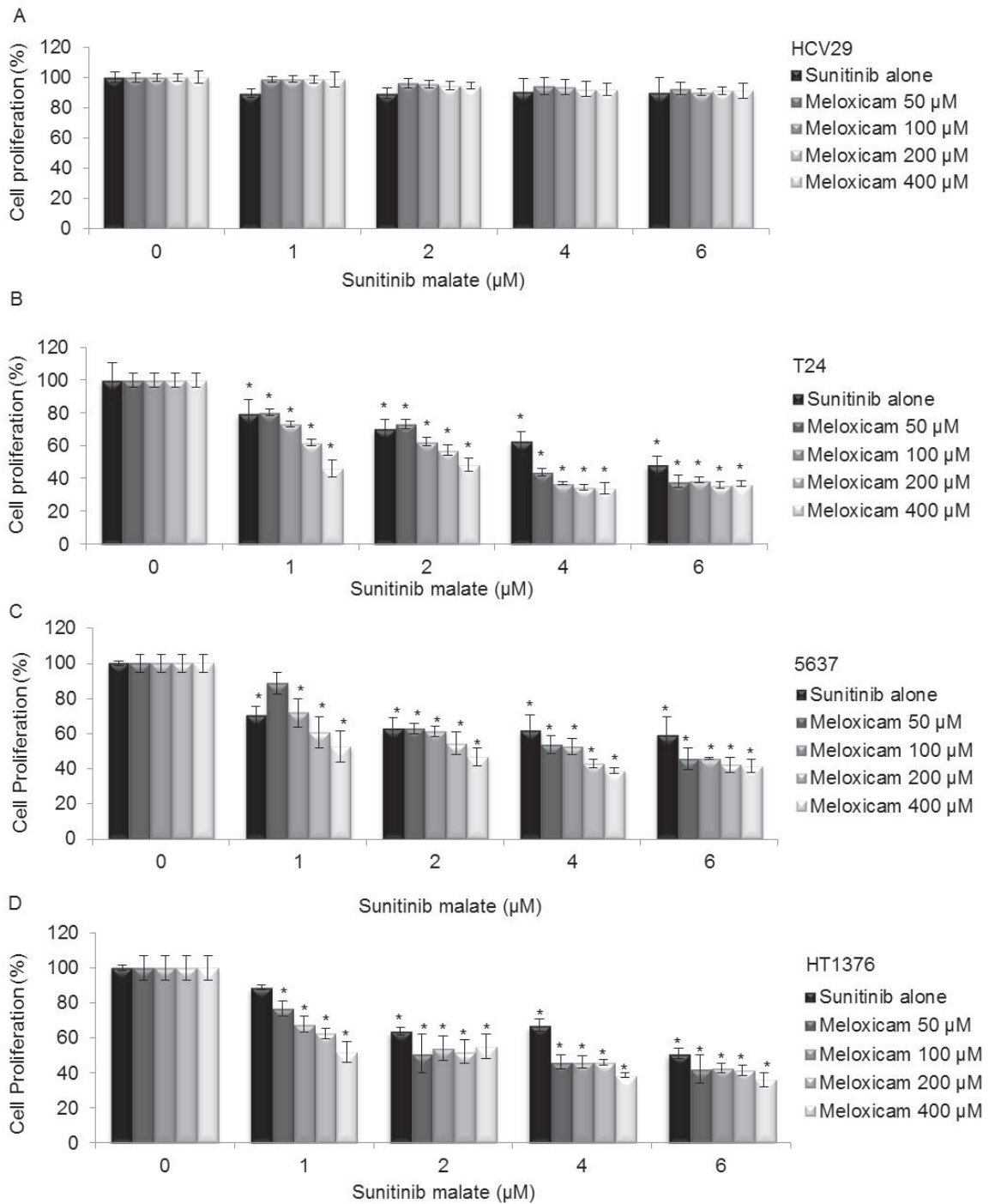


Fig. 3. Combined effects of sunitinib malate and meloxicam on (A) HCV29, (B) T24, (C) 5637 and (D) HT1376 bladder cells proliferation. The data shown and the bars represent the mean values \pm SD. * Statistical significant compared with untreated cells.

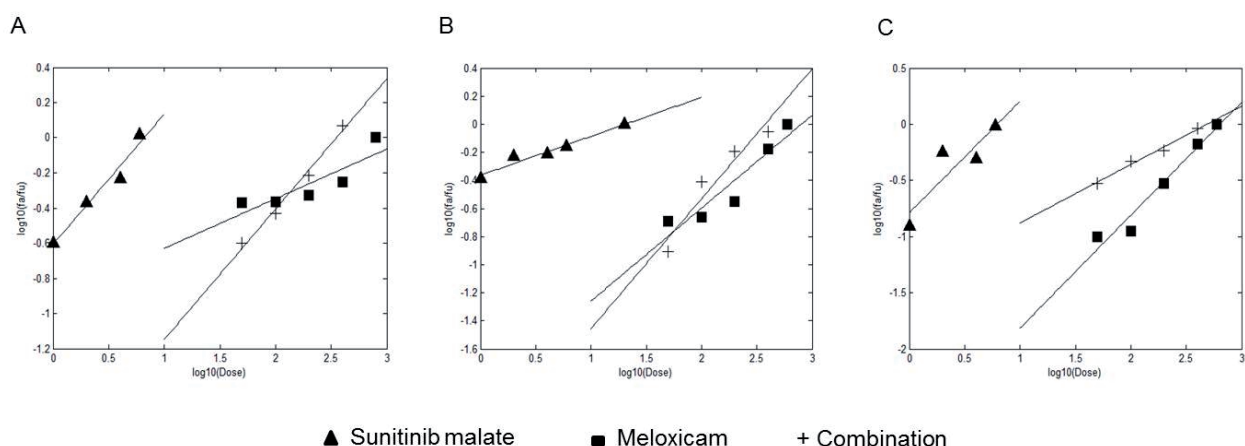


Fig. 4. Median-effect plot for sunitinib malate (1 μ M) and meloxicam (50, 100, 200 and 400 μ M) combination on (A) T24, (B) 5637 and (C) HT1376 bladder-cancer cell lines.

Evaluation of DNA damage

Comet assay was performed to assess the mechanism involved in the cytotoxic effects of sunitinib malate and meloxicam. The size of comet tail in untreated cells was very low, with approximately 10 A.U. in all the cell lines (Fig. 5A). This low level of damage in the control cells suggests that the assay was well-executed and that cells were in perfect condition for the assay. Similar results were obtained in sunitinib malate and meloxicam HCV29 treated cells, in isolation or combined. On the other hand, cells treated with sunitinib malate and meloxicam as single agents induced DNA damage in all the cancer cell lines. Comparing the DNA damage induced by each drug in isolation, sunitinib malate induces approximately 7% more DNA damage on the T24 cell line and 13% more in the other two cell lines than meloxicam. However, the highest intensity comet tail was observed when a combined treatment was applied: 1 μ M sunitinib malate plus 100 μ M meloxicam induced DNA damage on T24, 5637 and HT1376 cells of 101, 129 and 103 arbitrary units, respectively (Fig. 5B).

Detection of autophagy

In order to evaluate if sunitinib malate and meloxicam exposure induces the development of autophagosomes, HCV29, T24, 5637 and HT1376 cells were stained with MDC, a marker of autophagic vacuoles. Under a fluorescence microscope, autophagic vacuoles are visualized as distinct dot-

like structures dispersed in the cytoplasm or in the perinuclear regions. HCV29 untreated and treated cells did not present autophagic vacuoles. MDC-labelled vesicles were detected after 72 h of treatment with sunitinib malate and meloxicam, in isolation, in the three bladder-cancer cell lines (Fig. 6). In the simultaneous schedule, an increased number of MDC-labelled vesicles (fluorescence particles) were observed. Cells cultured in the culture medium only did not present autophagic vacuoles.

Detection of early stages of apoptosis

The M30 CytoDEATH antibody was applied to assess the caspase-cleaved epitope of cytokeratin 18, which is exposed during the early phase of the apoptotic event. HCV29 untreated and treated cells did not show positive staining, with a good pattern of proliferation. The presence of T24, 5637 and HT1376 bladder-cancer cells with positive staining was very similar between the different cell types after exposure to sunitinib malate (1 μ M) or meloxicam (100 μ M), in isolation, with two or three positive cells per field of visualization. However, when using the combined therapy, a noticeable number of positive cells were observed in the three cell lines with four or five cells showing positive staining per field of visualization (Fig. 7). Untreated cells did not show positive staining, with a good pattern of proliferation, as is shown by the presence of several dividing cells.

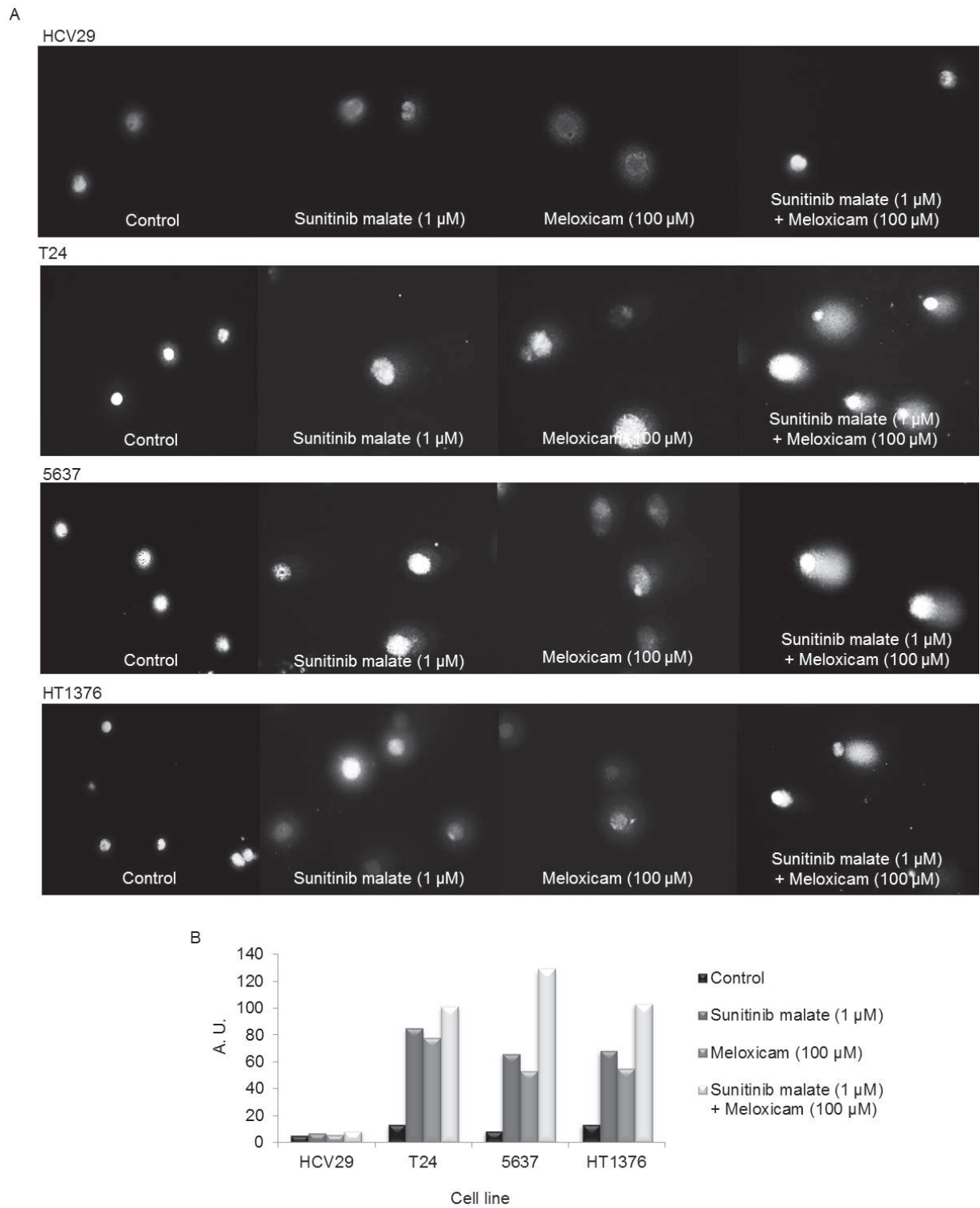


Fig. 5. (A) DNA damage on HCV29, T24, 5637 and HT1376 cells, after treatment with sunitinib malate (1 μ M) and meloxicam (100 μ M), in isolation or combined treatment; (B) Arbitrary units obtained after treatment. Original magnification 400 \times .

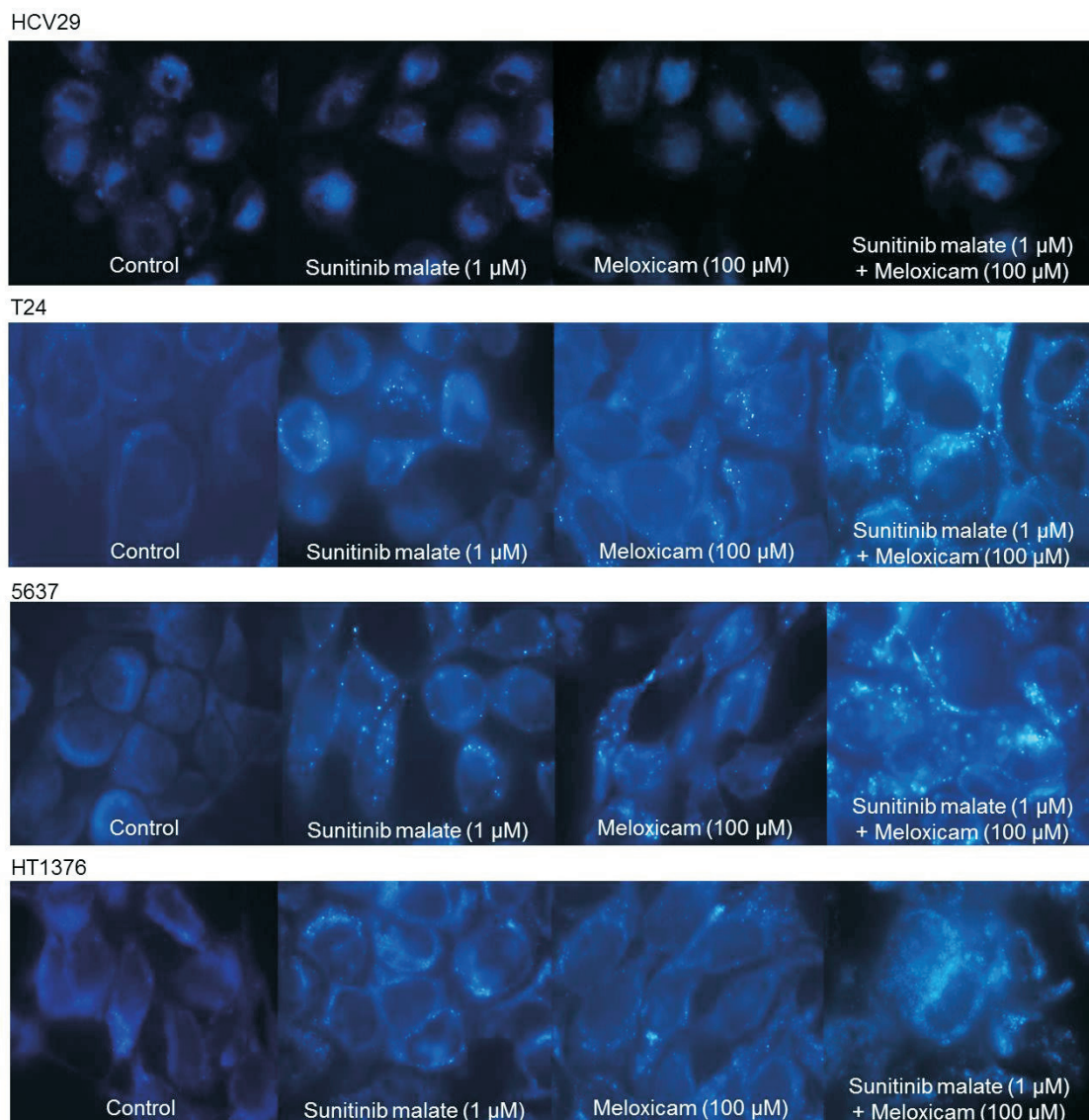


Fig. 6. **Representative photomicrographs of autophagic vacuoles stained with MDC** on HCV29, T24, 5637 and HT1376 cell lines. Bladder cells were incubated in the absence (control) and in the presence of sunitinib malate (1 μ M) and meloxicam (100 μ M). Original magnification 400 \times .

DISCUSSION

This study aims to provide information on the effects of meloxicam on bladder-cancer cells in isolation and when combined with sunitinib malate. To our knowledge, this is the first report in which meloxicam activity is analysed on human bladder-cancer cell lines.

Data compiled thus far suggests that the efficacy of conventional anti-cancer agents can be enhanced by their use in combination with NSAIDs (Hida et al. 2000, Awara et al. 2004, Mizutani et al. 2004, Naruse

et al. 2007). The efficacy of selective COX-2 inhibitors, combined with tyrosine kinase inhibitors, has also been observed (Chen et al. 2008). We have found an increase of apoptotic cells when compared with the control cells. Also, a statistically significant inhibition of cell proliferation in a concentration-dependent manner was observed in the three cell lines compared with untreated cells. Similar results were observed by Naruse et al. (2007) on human MG-63 osteosarcoma cells and in other malignant models (Kern et al. 2004, Wolfesberger et al. 2006).

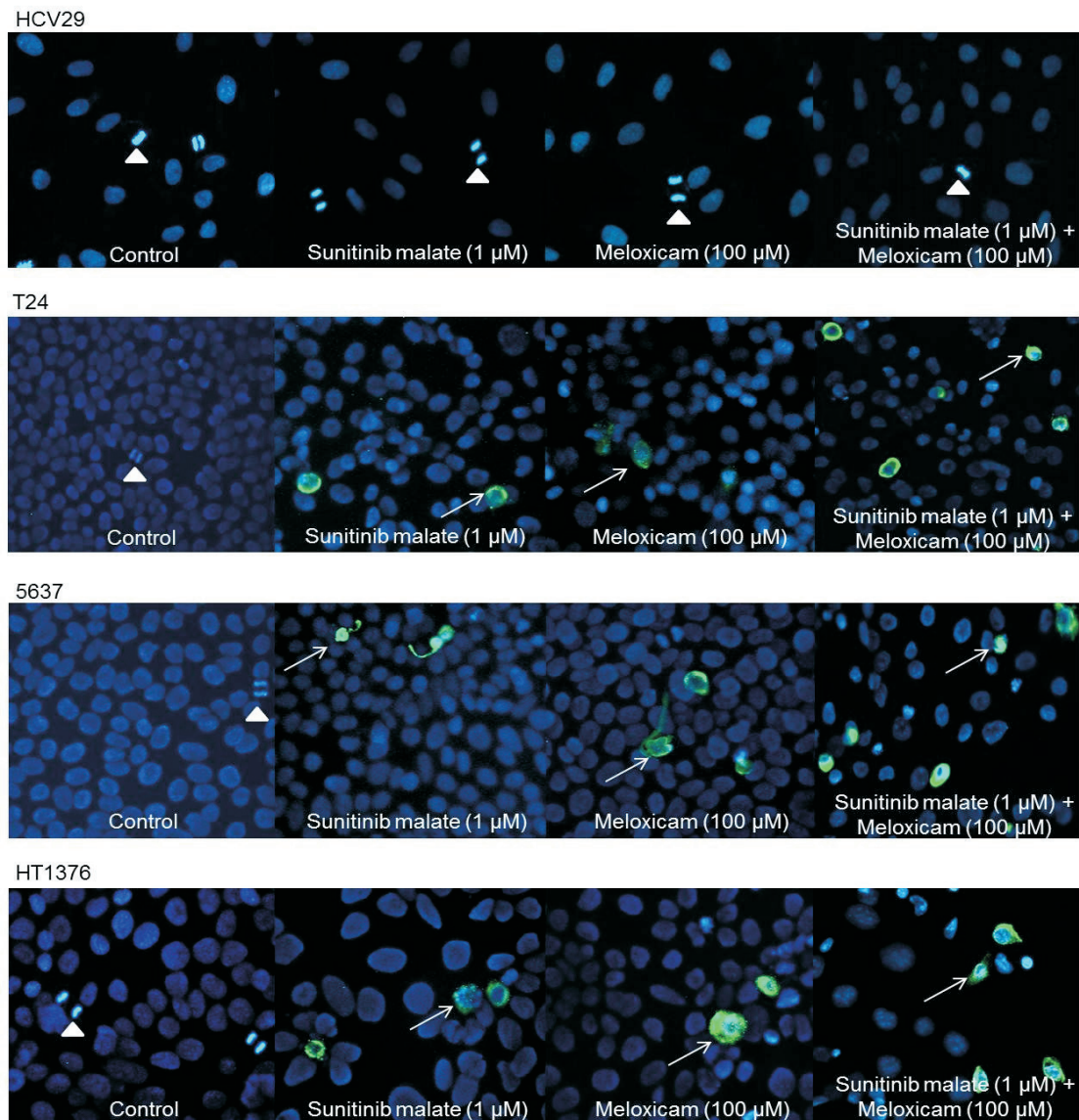


Fig. 7. Immunofluorescence analysis generated by M30 CytoDEATH antibody highlighting caspase cleaved cytokeratin 18. Occurrence of mitosis is shown by a white arrow head. Apoptotic cells (white arrow) are visualized by fluorescein isothiocyanate (FITC) colour (original magnification 200×).

The activity of sunitinib malate has already been demonstrated in *in vivo* studies, with concentration and time-dependent anti-tumour effects observed on the growth of mice's small lung cells (Abrams et al. 2003) and colon xenografts (Morimoto et al. 2003), as well as in *in vitro* studies, including on 5637, TCC-SUP, HTB5, HTB9, T24, UMUC14, SW1710 and J82 bladder-cancer cell lines (Cuneo et al. 2008, Sonpavde et al. 2009, Pan et al. 2011, Verbeek et al. 2011, Yoon et al. 2011). In this study, no different results were obtained on T24, 5637 and HT1376 bladder-cancer cell lines when using

sunitinib malate, as shown by the presence of apoptotic cells detected by morphological analysis. MTT assay, a versatile method of evaluating cell proliferation, showed a significant concentration-dependent anti-tumour activity in the three cell lines, after 72 h of exposure.

On the other hand, a synergistic interaction ($CI < 1$) with a combined schedule of sunitinib malate and meloxicam was obtained in T24, 5637 and HT1376 bladder-cancer cell lines. The other biological approaches used confirmed this result. Therefore, in the comet assay, that allows the analysis of breaks in

double- and single-stranded DNA (Collins 2004), we detected a major incidence in the combined treatment, which was lower with sunitinib malate and even lower still with meloxicam. It is also important to note that DNA damage obtained in untreated cells (approximately 10 A.U.) suggests that cells were in perfect condition for the assay.

When associated with a decrease in cell proliferation, there is an increase in cell death by autophagy or apoptosis. Recently, autophagy has been associated with a genetically programmed pathway that promotes cell death and with an important effect on cancer (Cuervo 2004, Kondo et al. 2005). Munafó and Colombo (2001) introduced MDC staining as a marker to detect autophagy. Sunitinib malate as a single agent led to a moderate induction of autophagic vacuoles in the three cell lines, when compared to untreated cells which did not show labelled vacuoles, as described by Zhao et al. (2010). Autophagy was induced by meloxicam, a COX-2 inhibitor, as has been observed by others (Huang and Sinicrope 2010). In this study, meloxicam in combination with sunitinib malate had an enhanced effect, with a marked increase of labelled vacuoles.

Apoptosis is also another pathway with a specific morphological pattern of programmed death (Fink and Cookson 2005). It was found that the combination of both drugs increased the number of early apoptotic cells in the three cell lines, compared to the use of the drugs in isolation.

In conclusion, a synergistic effect on non-muscle-invasive bladder tumour cell line 5637 and muscle-invasive bladder tumour cell lines T24 and HT1376 was obtained with the combined treatment. These effects were underlined by reduced cell proliferation, increased DNA damage, autophagy and early apoptosis. These results clearly demonstrate that both drugs were effective. However, this evidence does not necessarily translate into efficacy, i.e., we can only see an effect for which our assay was specifically designed. If a substance gives good results when tested it does not necessarily mean that this substance is effective (Berger 2011, Drell et al. 2012). Taking this into consideration, it is absolutely necessary to establish guidelines for performing *in vitro* studies, in order to create a basic framework with good predictive properties, but until now this had not been done (Drell et al. 2012, Kooijman et al. 2012). The impossibility of tumour angiogenesis and metastasis studies can be considered as limitations of *in vitro* studies, since these are complex processes with different mechanisms involved. It is therefore clearly difficult to perform *in vitro* assays which totally simulated these processes. It is probable that only a combination of methods will provide a clear picture (Drell et al. 2012). *In vitro* studies can also provide important information concerning the parameters of

pharmacodynamics. However, to better understand pharmacokinetics, it is necessary to use *in vivo* models, since these models offer the best approach for effectively combining and interpreting the major determinants of drug action across species (Mager et al. 2009). Likewise, *in vitro* studies do not predict the adverse effects of drugs (Kooijman et al. 2012).

ACKNOWLEDGEMENTS

This study was supported by an grant from the Fundação para a Ciência e Tecnologia, Ministério da Educação, Portugal, grant number SFRH/BD/47612/2008 and financed by FCT Pest-OE/AGR/UI0772/2011 unity. The authors express their deepest appreciation to Professor Ana Maria Nazaré of the University of Trás-os-Montes and Alto Douro, by the availability of the Elisa reader, to Dr. Maria Luis Cardoso, of the Faculty of Pharmacy of Porto, for his review of the manuscript and to Professor Jorge Colaço of the University of Trás-os-Montes and Alto Douro, for his contribution on statistical analysis.

REFERENCES

- Abrams TJ, Lee LB, Murray LJ, Pryer NK, Cherrington JM. SU11248 inhibits KIT and platelet-derived growth factor receptor beta in preclinical models of human small cell lung cancer. *Mol Cancer Ther.* 2: 471–478, 2003.
- Awara WM, El-Sisi AE, El-Sayad ME, Goda AE. The potential role of cyclooxygenase-2 inhibitors in the treatment of experimentally-induced mammary tumour: does celecoxib enhance the anti-tumour activity of doxorubicin? *Pharmacol Res.* 50: 487–498, 2004.
- Bellmunt J, González-Larriba JL, Prior C, Maroto P, Carles J, Castellano D, Mellado B, Gallardo E, Perez-Gracia JL, Aguilar G, Villanueva X, Albanell J, Calvo A. Phase II study of sunitinib as first-line treatment of urothelial cancer patients ineligible to receive cisplatin-based chemotherapy: baseline interleukin-8 and tumor contrast enhancement as potential predictive factors of activity. *Ann Oncol.* 22: 2646–2653, 2011.
- Berger J. The age of biomedicine: current trends in traditional subjects. *J Appl Biomed.* 9: 57–61, 2011.
- Chandrasekharan NV, Dai H, Roos KL, Evanson NK, Tomsik J, Elton TS, Simmons DL. COX-3, a cyclooxygenase-1 variant inhibited by acetaminophen and other analgesic/antipyretic drugs: cloning, structure, and expression. *Proc Natl Acad Sci USA.* 99: 13926–13931, 2002.

- Chen L, He Y, Huang H, Liao H, Wei W. Selective COX-2 inhibitor celecoxib combined with EGFR-TKI ZD1839 on non-small cell lung cancer cell lines: *in vitro* toxicity and mechanism study. *Med Oncol*. 25: 161–171, 2008.
- Chou TC, Talalay P. Quantitative analysis of concentration-effect relationships: the combined effects of multiple drugs or enzyme inhibitors. *Adv Enzyme Regul*. 22: 27–55, 1984.
- Collins AR. The Comet Assay for DNA Damage and Repair: Principles, Applications, and Limitations. *Mol Biotechnol*. 26: 249–461, 2004.
- Collins AR, Oszcoz AA, Brunborg G, Gaivão I, Giovannelli L, Kruszewski M, Smith CC, Stetina R. The comet assay: topical issues. *Mutagenesis*. 23: 143–151, 2008.
- Compare D, Nardone O, Nardone G. Non-Steroidal Anti-Inflammatory Drugs in the Carcinogenesis of the Gastrointestinal Tract. *Pharmaceuticals*. 3: 2495–2516, 2010.
- Cuervo AM. Autophagy: in sickness and in health. *Trends Cell Biol*. 14: 70–77, 2004.
- Cuneo KC, Geng L, Fu A, Orton D, Hallahan DE, Chakravarthy AB. SU11248 (sunitinib) sensitizes pancreatic cancer to the cytotoxic effects of ionizing radiation. *Int J Radiat Oncol Biol Phys*. 71: 873–879, 2008.
- Dhawan D, Jeffreys AB, Zheng R, Stewart JC, Knapp DW. Cyclooxygenase-2 dependent and independent antitumor effects induced by celecoxib in urinary bladder cancer cells. *Mol Cancer Ther*. 7: 897–904, 2008.
- Drell TL 4th, Zanker KS, Entschladen F. Translational research in oncology: The need of additional *in vitro* preclinical testing methods for new drugs. *Curr Pharm Des*. 18: 3416–3420, 2012.
- Eberhart CE, Coffey RJ, Radhika A, Giardiello FM, Ferrenbach S, DuBois RN. Up-regulation of cyclooxygenase 2 gene expression in human colorectal adenomas and adenocarcinomas. *Gastroenterology*. 107: 1183–1188, 1994.
- Fink SL, Cookson BT. Apoptosis, pyroptosis, and necrosis: mechanistic description of dead and dying eukaryotic cells. *Infect. Immun*. 73: 1907–1916, 2005.
- Furst DE. Meloxicam: Selective COX-2 inhibition in clinical practice. *Semin Arthritis Rheum*. 26: 21–27, 1997.
- Gallagher DJ, Milowsky MI, Gerst SR, Ishill N, Riches J, Regazzi A, Boyle MG, Trout A, Flaherty AM, Bajorin DF. Phase II study of sunitinib in patients with metastatic urothelial cancer. *J Clin Oncol*. 28: 1373–1379, 2010.
- Goldman AP, Williams CS, Sheng H, Lamps LW, Williams VP, Pairet M, Marrow JD, DuBois RN. Meloxicam inhibits the growth of colorectal cancer cell. *Carcinogenesis*. 19: 2195–2199, 1998.
- Gupta S, Srivastava M, Ahmad N, Bostwick DG, Mukhtar H. Overexpression of cyclooxygenase-2 in human prostate adenocarcinoma. *Prostate*. 42: 73–78, 2000.
- Hamama AK, Ray J, Day RO, Brien JE. Simultaneous Determination of Rofecoxib and Celecoxib in Human Plasma by High-Performance Liquid Chromatography. *J Chromatogr Sci*. 43: 351–354, 2005.
- Hida T, Kozaki K, Muramatsu H, Masuda A, Shimizu S, Mitsudomi T, Sugiura T, Ogawa M, Takahashi T. Cyclooxygenase-2 inhibitor induces apoptosis and enhances cytotoxicity of various anticancer agents in non-small cell lung cancer cell lines. *Clin Cancer Res*. 6: 2006–2011, 2000.
- Huang S, Sinicrope FA. Celecoxib-induced apoptosis is enhanced by ABT-737 and by inhibition of autophagy in human colorectal cancer cells. *Autophagy*. 6: 256–269, 2010.
- Hwang D, Scollard D, Byrne J, Levine E. Expression of cyclooxygenase-1 and cyclooxygenase-2 in human breast cancer. *J Natl Cancer Inst*. 90: 455–460, 1998.
- Jacobs BL, Montgomery JS, Zhang Y, Skolarus TA, Weizer AZ, Hollenbeck BK. Disparities in bladder cancer. *Urol Oncol*. 30: 81–88, 2012.
- Karin M. Nuclear factor- κ B in cancer development and progression. *Nature*. 441: 431–436, 2006.
- Kern MA, Schöneweiss MM, Sahi D, Bahlo M, Haugg AM, Kasper HU, Dienes HP, Käferstein H, Breuhahn K, Schirmacher P. Cyclooxygenase-2 inhibitors suppress the growth of human hepatocellular carcinoma implants in nude mice. *Carcinogenesis*. 25: 1193–1199, 2004.
- Kondo Y, Kanzawa T, Sawaya R, Kondo S. The role of autophagy in cancer development and response to therapy. *Nature Rev Cancer*. 5: 726–734, 2005.
- Kooijman M, van Meer PJ, Moors EH, Schellekens H. Thirty years of preclinical safety evaluation of biopharmaceuticals: did scientific progress lead to appropriate regulatory guidance? *Expert Opin Drug Saf*. 11: 797–801, 2012.
- Mager DE, Woo S, Jusko WJ. Scaling pharmacodynamics from *in vitro* and preclinical animal studies to humans. *Drug Metab Pharmacokinet*. 24: 16–24, 2009.
- Michaud DS. Chronic inflammation and bladder cancer. *Urol Oncol*. 25: 260–268, 2007.
- Mizutani Y, Nakanishi H, Li YN, Sato N, Kawauchi A, Miki T. Enhanced sensitivity of bladder cancer cells to cisplatin mediated cytotoxicity and apoptosis *in vitro* and *in vivo* by the selective cyclooxygenase-2 inhibitor JTE-522. *J Urol*. 172: 1474–1479, 2004.

- Montejo C, Barcia E, Negro S, Fernández-Carballido A. Effective antiproliferative effect of meloxicam on prostate cancer cells: Development of a new controlled release system. *Int J Pharm.* 387: 223–229, 2010.
- Morimoto AM, Tan N, West K, McArthur G, Toner GC, Manning WC, Smolich BD, Cherrington JM. Gene expression profiling of human colon xenograft tumors following treatment with SU11248, a multitargeted tyrosine kinase inhibitor. *Oncogene.* 23: 1618–1626, 2003.
- Munafó DB, Colombo MI. A novel assay to study autophagy: regulation of autophagosome vacuole size by amino acid deprivation. *J Cell Sci.* 114: 3619–3629, 2001.
- Naruse T, Nishida Y, Ishiguro N. Synergistic effects of meloxicam and conventional cytotoxic drugs in human MG-63 osteosarcoma cells. *Biomed Pharmacother.* 61: 338–346, 2007.
- Pan F, Tian J, Zhang X, Zhang Y, Pan Y. Synergistic interaction between sunitinib and docetaxel is sequence dependent in human non-small lung cancer with EGFR TKIs-resistant mutation. *J Cancer Res Clin Oncol.* 137: 1397–1408, 2011.
- Ping SY, Wu CL, Yu DS. Sunitinib can enhance BCG mediated cytotoxicity to transitional cell carcinoma through apoptosis pathway. *Urol Oncol.* 30: 652–659, 2012.
- Scheiman JM, Hindley CE. Strategies to optimize treatment with NSAIDs in patients at risk for gastrointestinal and cardiovascular adverse events. *Clin Ther.* 32: 667–677, 2010.
- Sonpavde G, Jian W, Liu H, Wu MF, Shen SS, Lerner SP. Sunitinib malate is active against human urothelial carcinoma and enhances the activity of cisplatin in a preclinical model. *Urol Oncol.* 27: 391–399, 2009.
- Tsubouchi Y, Mukai S, Kawahito Y, Yamada R, Kohno M, Inoue K, Sano H. Meloxicam inhibits the growth of colorectal cancer cells. *Carcinogenesis.* 19: 2195–2199, 2000.
- Tsuchida A, Itoi T, Kasuya K, Endo M, Katsumata K, Auki T, Suzuki M, Aoki K. Inhibitory effect of meloxicam, a cyclooxygenase-2 inhibitor, on N-nitrosobis (2-oxopropyl) amine induced biliary carcinogenesis in Syrian hamsters. *Carcinogenesis.* 26: 1922–1928, 2005.
- Verbeek HH, Alves MM, de Groot JW, Osinga J, Plukker JT, Links TP, Hofstra RM. The effects of four different tyrosine kinase inhibitors on medullary and papillary thyroid cancer cells. *J Clin Endocrinol Metab.* 96: 991–995, 2011.
- Watkins DN, Lenzo JC, Segal A, Garlepp MJ, Thompson PJ. Expression and localization of cyclo-oxygenase isoforms in non-small cell lung cancer. *Eur Respir J.* 14: 412–418, 1999.
- Wiedenmann B, Pavel M, Kos-Kudla B. From targets to treatments: a review of molecular targets in pancreatic neuroendocrine tumors. *Neuroendocrinology.* 94: 177–190, 2011.
- Williams CS, Mann M, DuBois RN. The role of cyclooxygenases in inflammation, cancer, and development. *Oncogene.* 18: 7908–7916, 1999.
- Wolfesberger B, Hoelzl C, Walter I, Reider GA, Fertl G, Thalhammer JG, Skalicky M, Egerbacher M. *In vitro* effects of meloxicam with or without doxorubicin on canine osteosarcoma cells. *J Vet Pharmacol Ther.* 29: 15–23, 2006.
- Yoon CY, Lee JS, Kim BS, Jeong SJ, Hong SK, Byun SS, Lee SE. Sunitinib malate synergistically potentiates anti-tumor effect of gemcitabine in human bladder cancer cells. *Korean J Urol.* 52: 55–63, 2011.
- Zhao Y, Xue T, Yang X, Zhu H, Ding X, Lou L, Lu W, Yang B, He Q. Autophagy plays an important role in sunitinib-mediated cell death in H9c2 cardiac muscle cells. *Toxicol Appl Pharmacol.* 248: 20–27, 2010.